Chinese Science Bulletin

Vegetation change detection using artificial neural networks with ancillary data in Xishuangbanna, Yunnan Province, China

ZHANG ZhiMing[1,2], Lieven VERBEKE[2], Eva De CLERCQ[2], OU XiaoKun[1†] & Robert De WULF[2]

[1] Institute of Ecology and Geobotany, Yunnan University, Kunming 650091, China;
[2] Laboratory of Forest Management and Spatial Information, Ghent University, Ghent 9000, Belgium

Timely and accurate change detection of the Earth's surface features provides the foundation for better planning, management and environmental studies. In this study ANN change detection was used to perform vegetation change detection, and was compared with post-classification method. Before the post-classification was performed the ANN classification was used to yield multitemporal vegetation maps. ANN were also used to perform a one-pass classification for the images in 2003 and 2004. DEM and slope were used as two extra channels. During the training stage, the training data was separated into 82 subclasses including 36 change subclasses and 46 no change subclasses. Moreover NDVI differencing methods were used to develop the change mask. The result showed that combining the NDVI differencing method with visual interpretation when identifying reference areas can produce more accurate change detection results for the ANN one pass change classification. Moreover, it is effective to use elevation and slope as extra channels together with PCA components, to perform ANN-based change detection in mountainous study areas. It is also important to separate the vegetation transition classes into subclasses based on spectral response patterns, especially for mountainous terrains. This processing can reduce the topographic effect and improve the change detection accuracy.

ANN change detection, elevation data, vegetation change, post-classification, NDVI differencing

Land-use/cover change is one of the major drivers of changes in the structure, functioning, and dynamics of most ecosystem and landscapes throughout the world. Land-use/cover changes are caused by both natural processes and human activities[1-4]. Today, the study of causes, process, and consequences of land use/cover change is one of the main research topics of landscape ecology[5]. Timely and accurate change detection of the Earth's surface features provides the foundation for studying and understanding their causes, process and consequences. In addition, remote sensing data, because of their temporal resolution, synoptic view and digital format suitable for computer processing, have become the major data source for different change detection applications during the last decades.

Since the 1970s, a number of change detection techniques were developed for detecting land cover change and vegetation change[6-10]. Lu et al.[10] classified these techniques into seven categories: (1) algebra, (2) transformation, (3) classification, (4) advanced models, (5) Geographical Information System (GIS) approaches, (6) visual analysis, and (7) other approaches. These techniques are characterized by their functionalities and the data transformation procedures involved. Based on these characteristics, the current change detection techniques can be further grouped into two broad types[11]:

Received January 5, 2007; accepted April 10, 2007
doi: 10.1007/s11434-007-0711-1
†Corresponding author (email: xkou@ynu.edu.cn)
Supported by the National Key Project for Basic Research on Ecosystem Changes in Longitudinal Range-Gorge Region and Transboundary Eco-security of Southwest China (Grant No. 2003CB415102), Vlaamse Interuniversitaire Raad (VLIR ZEIN2002PR264-886), Belgium and Foundation of Provincial Education, Yunnan Province (Grant No. 04Y220B)

Change Mask Development (CMD): Only change and no-change are detected and no categorical change information can be directly provided.

Categorical Change Extraction (CCE): Complete categorical changes are extracted.

Among all these techniques, post-classification is a common approach used for change detection in practice, but the difficulty in classifying historical image data often seriously affects the change results. This method performs pixel-by-pixel comparison of two single-date classified images and generates a full change matrix. The performance of this technique critically depends on the accuracies of the individual classifications. The problem is the propagation of error inherited from each classification process.

The use of artificial neural networks (ANN) for change detection has received increasing attention. ANN have been used for land-cover change[11−14], forest mortality change[15], forest change[16] and urban change[17]. These studies suggest that the ANN method can improve the accuracy of change detection compared to post-classification comparison methods. In general, the ANN method is a direct multidate classification technique[11], based on a single analysis of a combined data set of two or more dates to identify changes. Each change combination between the two times is represented as an output class, and the change detection process is treated as one classification. To efficiently use this technique, it is necessary to identify sufficient training data in which each possible type of change is represented[18].

Although ANN change detection technique already was used to detect land-cover change, implementing accurate change detection for a specific mountain study area is still a challenge. Since in mountainous areas, the distribution of the vegetation is influenced by topographical factors, using topographic information could be helpful to improve the classification accuracy.

The objective of this study was to obtain an accurate vegetation change map in the study area, integrating elevation data and using the ANN change detection technique. These objectives raise the following research questions:

How to obtain enough data for each vegetation class and their transitions?

Can the accuracy of change detection be improved by ANN change detection when elevation and slope data are used as additional bands?

1 Study area and material

1.1 Study area

The study area in the Xishuangbanna prefecture of China's Yunnan Province is located at 22°00′−23°50′00″N and 100°00′12″−102°00′E and covers about 50000 ha. It belongs to the catchment of the Lancang River and is located in the Xishuangbanna Dai Autonomous Prefecture (Figure 1). Xishuangbanna is home to the richest biological and ethnic diversity in China.

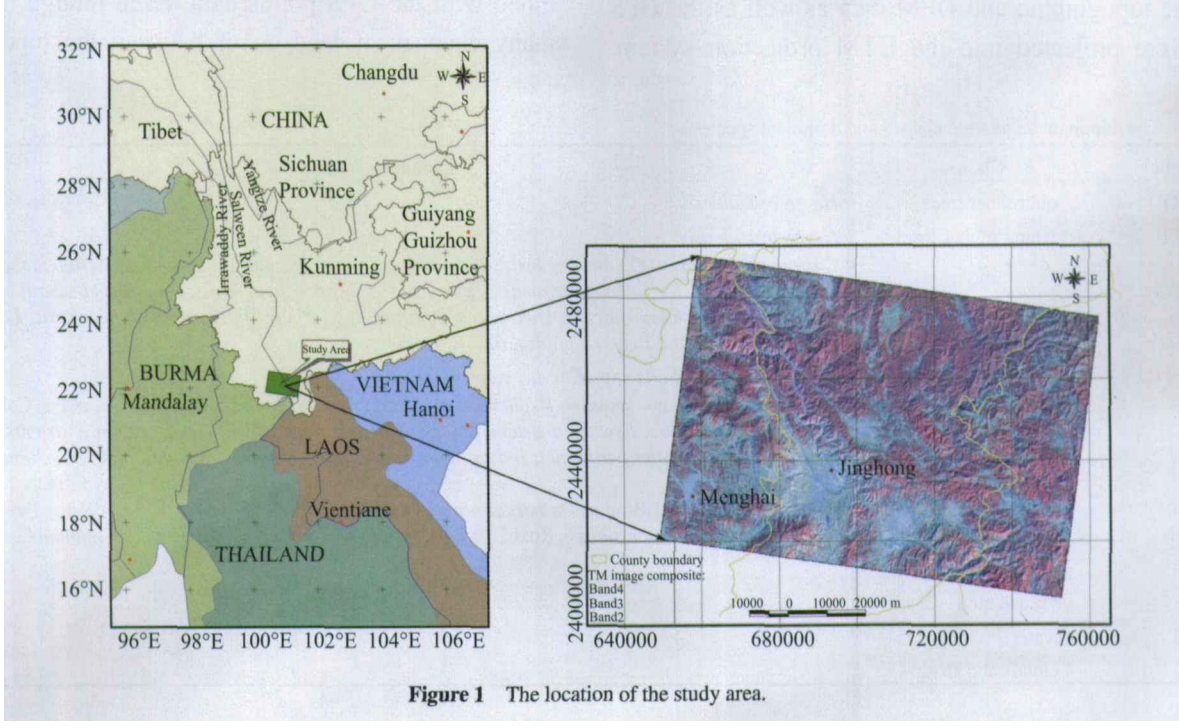

Figure 1 The location of the study area.

There are 14 different ethnic minorities that inhabit this tropical region of Yunnan. It is a mountainous area. The difference in altitude between the lowest to the highest peak is about 2000 m. The climate of the region is strongly seasonal with two main air masses alternating during the year. The average temperature is between 16.4℃ and 22.0℃. Between May and October the South-West Monsoon air mass brings about 80 % of annual rainfall, whereas the dry and cold air of the Southern edges of the jet stream dominates the climate between November and April. Annual rainfall varies between 1200 mm in the Mekong valley and 1900 mm at altitudes above about 1500 m. Although the rainfall is very seasonal, the dry season is not extreme in nature.

1.2 Satellite and reference data

The data includes two Landsat TM images (path/row: 130/45), a 1:100000 scale topographic map, 20 m resolution DEM data and GPS ground points. One image was acquired on March 7th, 2003 with a sun elevation of 50.49° and solar azimuth angle of 130.05° (Landsat 7 ETM+). Another was acquired on March 1st, 2004 with a sun elevation of 47.67° and solar azimuth angle of 130.65° (Landsat 5 TM). The images were projected into the Universal Transverse Mercator (UTM) projection system (zone number: 47, reference datum: WGS84). The topographic maps and DEM data were projected into the originally Gauss Kruger projection system, with the reference datum respectively Beijing 54 and Xi'an 80. The topographic and DEM data as well as the GPS data were projected into the UTM projection system. After the topographic maps and DEM data were projected, 25 control points were selected to perform a geometric correction using a fourth-degree polynomial. The Root Means Square (RMS) error between the DEM and the image was about 15 m. The Root Means Square (RMS) error for the two images was about 15 meters. For a more comprehensive discussion of the image data used in this study, the reader is referred to the report on "The accuracy assessment of the image geometric registration".

1.3 The vegetation classes in the study area

For this work, the Landsat TM and ETM+ image data will be used to perform vegetation change detection. Based on the preliminary classifications of the image data, the objective of the study and the drivers of vegetation change, 10 classes could be identified in the southern study area, including clouds and shadows (Table 1).

1.4 Validation and training data

492 GPS points, collected in March 2004, are located in the study area. For each point, the dominant species, canopy cover and height of the plant communities were recorded. However, most of the 492 points are located along riversides and roadsides. Few of them are located in mountainous and rural areas. In order to get enough training data for rural area, parts of the topographic map were also used as training data because a number of attribute values were suitable as ground truth data combined with the GPS points data. Even though there are many changes of land cover between the topographic

Table 1 The dominant vegetation classes and dominant species

Symbol	Classes	Dominant species
ORT	old rubber trees	*Hevea brasiliensis*
YRT	young rubber trees	*Hevea brasiliensis*
EF	evergreen forest	*Castanopsis hystrix*, *C. mekongensis*, *Lithocarpus truncatus*, *Litsea glutinosa*, *Actinodaphne henryi*, *Schima wallichii*, *Syzygium yunnanensis*, *Elaeocarpus austro-yunnanensis*, *Paramichelia baillonii*, *Engelhardtia* spp., *Machilus salicina*, *Olea rosea*, *Aporusa* spp., *Pinus khasya* var. *langbianensis*, *Lithocarpus* sp., *Quercus dentata*, *Betula alnoides*, etc.
LDF	low density forest	*Pinus yunanensis*, *Salix* spp., *Corylus yunnensis* etc.
DF	deciduous forest	*Ficus altissima*, *Toona sinensis*, *Nephelium chryseum*, *Altingia excelsa*, *Bischofia javanica*, *Colona floribunda*, *Bombax ceiba*, *Erythrina stricta*, and *Bauhinia variegata* etc. *Dendrocalamus strictus*, *D. brandisii*, *Cephalostachyum pergracile*, *Indosasa sinica*, *Schizostachyum funghomii*, and *Dinochloa puberula* etc.
SGL	shrub and grass land	*Trema orientalis* (L.) Blume, *Dalbergia obtusifolia* (Baker) Prain, *Docynia indica* (Wall.) Decne. *Eurya groffii* Merr., *Saccharum sinense* Roxb., *Leucosceptrum canum* Sm., *Eupatorium coelestinum* L. etc.
AL	agriculture land	
BL	burned land	
WT	water	
CS	clouds and shadows	

maps and TM image, the plant community's types did not change notably, especially for the remote mountainous areas. The two images are only one year different. Combining the topographic maps with TM images and field ecological expertise, the training sites for each type of the vegetation were selected in the study area.

Because of the topographic effect in mountainous areas, the same vegetation class can show different spectral reflectance patterns in different aspects and slopes. In the ground truth digitizing stage, it is necessary to differentiate the ground truth data for each different signature class, even if they belong to the same vegetation class. There exist, for example, "oak forest on shaded slopes", "oak forest on sunny slopes", "old rubber trees" and "young rubber trees". In any case, the classification accuracy will generally be improved if each spectral class or subclass is treated as a separate category[19]. 48 subclasses were digitized for the image in 2003, and 46 subclasses were digitized for the image in 2004. The ground truth polygons were converted into a raster map with a cell size of 30m × 30m. Then, this map was randomly divided into training set, test set and validation set. The test set was used for testing the error between the desired outputs and the actual network outputs calculation. The validation data was used for the accuracy assessment. After the classification was performed, the subclasses were merged into 10 vegetation classes based on the ancillary data (GPS points, topographic maps and DEM data, etc.) and field ecological expertise (Table 1).

To obtain the training data for the change vegetation classes, NDVI differencing was used to develop a change mask. Based on the location of change areas, field knowledge and visual inspection, 36 change sub-classes were extracted (Table 2). Because the two images were only one year different, some vegetation class transitions were not present, as confirmed after visual inspection. Based on field survey and visual inspection, even though the two images were collected in the same season (March), some changes were caused by different climate circumstances (Table 2). 82 subclasses, including the subclasses for the no-change areas, were digitized on the two images. After the ANN classification was executed, the subclasses were merged into 24 classes (Table 3).

1.5 Change detection methods

1.5.1 NDVI differencing. Vegetation indices have long been used in remote sensing for monitoring temporal changes associated with vegetation. Lyon et al.[20] compared seven vegetation indices from three different dates of MSS image data for land cover change detection and concluded that the NDVI differencing technique demonstrated the best vegetation change detection. In this study, NDVI differencing methods were used to develop the change mask. This mask was used to collect training data with TM band 5, 4 and 3 composite images by visual interpretation (Table 2).

1.5.2 Post-classification. Post-classification is the most obvious method of change detection, comparing two independently produced classified images. By properly coding the classification results for time t_1 and t_2, the analyst can produce change maps showing a complete matrix of changes[6]. In addition, selective grouping of classification results allows the analyst to observe any subset of change which may be of interest[6]. In this post-classification change detection technique, each image was classified using ANN classification, as described above.

In this study, after the ANN classification technique was performed for two individual images, 10 classes were retained. Before the post-classification was performed, clouds and shadows were masked. Then, 81 (9×9) classes were derived. Because the two images only have a one year difference, some changes did not occur. There are, for example, no "shrub and grass land to evergreen forest", "farm land to evergreen forest", "farm land to old rubber trees" and "burned land to old rubber trees. Based on field knowledge and after visual interpretation, the 81 classes were merged into 24 classes (Table 3).

1.5.3 ANN change detection. Artificial Neural Networks (ANN) have been widely used in remote sensing applications for the past decade (Figure 2). Normally, the simple neural network consists of three different types of layers: the units whose activations are the problem input for the network are called input layer; the units whose output represent the output of the network are referred to as output layer; the remaining units are called hidden layer, because they are not perceptible from the outside[21]. One of the main advantages of neural networks for classification is that they are independent of the distribution of the class-specific data in feature space. It is therefore possible for a single class to be represented in feature space as a series of clusters (rather than a single cluster)[22,23]. In addition, ANN change detection allows easy integration with ancillary data, such as field survey data and DEM data.

Table 2 The training data sets for change areas extracted after CMD and visual interpretation

Class	Land transition	Description	Number of training pixel
47	LDF to AL1	low density forest changed into agriculture land 1	623
48	EF to AL1	evergreen forest changed into agriculture land 1	950
49	LDF to BL	low density forest changed into burned land	2370
50	SGL to AL1	shrub and grass land changed into agriculture land 1	178
51	DF to DF without leaves	deciduous forest loosed leaves	1850
52	WT to AL2	water area changed into agriculture land 2	120
53	SGL to BL	shrub and grass land changed into burned land	2954
54	DF to BL	deciduous forest changed into burned land	2524
55	LDF to shaded SGL	low density forest change into shaded shrub and grass land	518
56	LDF to SGL	low density forest changed into shrub and grass land	374
57	BL to SGL	burned land changed into shrub and grass land	761
58	YRT to YRT without leaves 1	youngest rubber trees loosed their leaves	1155
59	EF to BL	evergreen forest changed into burned land	3217
60	EF to shaded EF	evergreen forest on shaded slopes	90
61	EF to LDF	evergreen forest changed into low density forest	291
62	YRT to YRT without leaves 2	young rubber trees loosed their leaves	2187
63	AL1 to BL	agriculture land 1 changed into burned land	300
64	EF to AL2	evergreen forest changed into agriculture land 2	916
65	SGL to AL2	shrub and grass land changed into agriculture land 2	208
66	EF to SGL	evergreen forest changed into shrub and grass land	1833
67	LDF to AL2	low density forest changed into agriculture land 2	707
68	DF to AL1	deciduous forest changed into agriculture land 1	1625
69	ORT to ORT without leaves	old rubber trees loosed their leaves	1640
70	ORT to AL2	old rubber trees changed into agriculture land 2	358
71	AL1 to AL2	agriculture land 1 changed into agriculture land 2	355
72	AL3 to AL4	agriculture land 3 changed into agriculture land 4	446
73	BL to BM	burned land changed into bamboo	538
74	AL2 to SGL	agriculture land 2 to shrub grass land	371
75	EF to shaded SGL	evergreen forest changed into shaded shrub and grass land	1847
76	EF to YRT	evergreen forest changed into young rubber trees	811
77	YRT to AL2	young rubber trees changed into agriculture land 2	578
78	BL to AL3	burned land changed into agriculture land 3	255
79	SGL to YRT	shrub and grass land changed into young rubber trees	159
80	BL to AL2	burned land changed into agriculture land 2	215
81	ORT to AL1	older forest changed into agriculture land 1	108
82	SGL2 to SGL2 without leaves	shrub and grass land loosed leaves	121
Total			33553

Table 3 The final classes for vegetation change map between 2003 and 2004

1	2	3	4	5	6	7	8	9	10	11	12
ORT-ORT	YRT-YRT	EF-EF	LDF-LDF	DF-DF	WT-WT	AL-AL	SGL-SGL	BL-SGL	LDF-AL	EF-AL	LDF-BL
13	14	15	16	17	18	19	20	21	22	23	24
SGL-BL	DF-BL	LDF-SGL	BL-LDF	EF-BL	SGL-AL	YRT-AL	EF-SGL	ORT-AL	BL-AL	YRT-ORT	BL-BL

Note: ORT-ORT, old rubber trees unchanged; YRT-YRT, young rubber trees unchanged; EF-EF, evergreen forest unchanged; LDF-LDF, low density forest unchanged; DF-DF, deciduous forest unchanged; WT-WT, water areas unchanged; AL-AL, agriculture land unchanged; SGL-SGL, shrub and grass land unchanged; BL-BL, burned land unchanged; BL-SGL, burned land changed into shrub and grass land; LDF-AL, low density forest changed into agriculture land; EF-AL, evergreen forest changed into agriculture land; LDF-BL, low density forest changed into burned land; SGL-BL, shrub and grass land changed into burned land; DF-BL, deciduous forest changed into burned land; LDF-SGL, low density forest changed into shrub and grass land; BL-LDF, burned land changed into low density forest; EF-BL, evergreen forest changed into burned land; SGL-AL, shrub and grass land changed into agriculture land; YRT-AL, young rubber trees change into agriculture land; EF-SGL, evergreen forest changed into shrub and grass land; ORT-AL, old rubber trees changed into agriculture land; BL-AL, burned land changed into agriculture land; YRT-ORT, young rubber trees changed into old rubber trees.

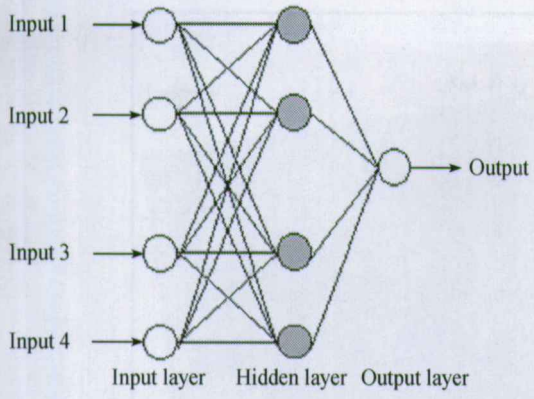

Figure 2 A simple neural network diagram (http://www.stowa-nn.ihe.nl/ANN.htm).

In this study three layer neural networks were constructed (input layer, hidden layer and output layer). ANN were used to perform a one-pass classification for the images in 2003 and 2004. The input layer has 16 neurons; representing 7 channels of TM image of 2004 and 7 channels of the image of 2003, DEM and slope were used as two extra channels. The number of neurons in the output layer is equal to the number of subclasses (82). The 82 subclasses include 36 change subclasses (Table 2) (and 46 no change subclasses). The number of the hidden neurons is 20. A sigmoid activation function was used in this neural network. The learning rate of this network is 0.001; the parameter of the momentum is 0.2. After the ANN classification was performed, the 82 subclasses were merged into 24 classes (Table 3). Additionally, in order to test the added value of elevation and slope as extra input channels, an ANN with 14 inputs was used.

Principal component analysis (PCA) was applied to extract the salient features from the input data and to discard noise, which hampers the ANN's learning[24]. The purpose of PCA is to reduce an original n-dimension data into fewer than n "new dimensions" or components, allowing for a smaller ANN architecture[25]. In this study, PCA was used to reduce the 14 TM channels into 8 PCA components. Then, ANN classification was performed with 8 PCA components, DEM and slope as input nodes and 82 subclasses as output nodes.

The implementation of the feed-forward neural networks algorithm was handled by a software tool developed in the Laboratory of Forest Management and Spatial Information Techniques (http://dfwm.ugent.be/forman).

1.6 Accuracy assessment

Accuracy assessment is very important for understanding the obtained results and for interpreting results in a decision-making context[10]. However, evaluating the accuracy of land cover or vegetation change detection by using multi-temporal, digital, remote sensing data is a considerable challenge[26]. In this study, the error matrix was also used to assess the accuracy of the vegetation change in the study area[27]. Firstly, the modified error matrix was used to evaluate the accuracy of post-classification change detection. As mentioned above, the recording dates of the two images are only one year different and the vegetation change map with 81 classes was merged into 24 classes. These 24 classes were used to calculate the error matrix. The same validation data were also used to evaluate the accuracy of the change vegetation map derived by using ANN-based change detection techniques. Secondly, in order to further analyze whether errors are due to misclassification or are caused by failures in the change detection techniques, the change detection error matrix is collapsed into a no-change/change error matrix. A no-change/change error matrix was also used to assess the accuracy of the NDVI differencing change detection method.

2 Results

2.1 Results from change detection methods

Post-classification change detection was performed on ANN classifications of the 2003 and 2004 images. Post-classification produced a cross-classification image and a transition matrix (Figure 3 and Table 4).

The vegetation classes were described in detail in the report of "The definition of vegetation classes in Xishuangbanna study area". Table 4 and Figure 5 show the vegetation changes occurring between 2003 and 2004. As mentioned above, some changes could not happen in one year. These are, for example, "old rubber trees to young rubber trees", "old rubber trees to evergreen forest", "evergreen forest to deciduous forest" and "water to evergreen forest", etc. (Table 4). After the error matrix was calculated, the overall accuracy was found to be 65.04% and the kappa value 0.6094 (Table 5).

Table 5 presents the overall accuracies and the Kappa values of the different change detection strategies. The poorest accuracy was generated by change detection 1 (post-classification with 81 full set of transition classes). The overall accuracy was 65.06%, and kappa value was 0.6096. However, after the 81 full sets of transition

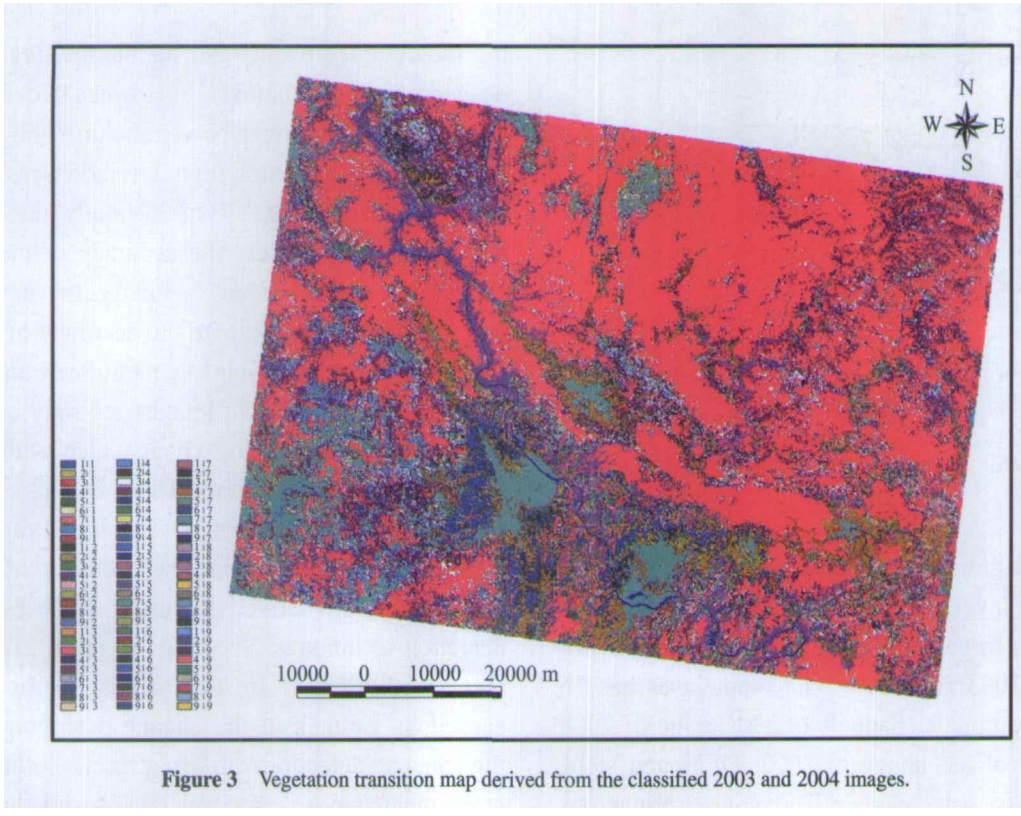

Figure 3 Vegetation transition map derived from the classified 2003 and 2004 images.

Table 4 Vegetation transition matrix between 2003 and 2004

2004 \ 2003	ORT	YRT	EF	LDF	DF	WT	AL	SGL	BL	Total (pixels)
ORT	126267	36538	24574	1926	49721	314	19839	1954	414	261547
YRT	66393	332985	63908	63849	151372	3458	120382	101413	14439	918199
EF	34332	8829	3161420	134630	108126	4543	16851	8380	4709	3481820
LDF	6820	17446	334149	470889	57982	356	62529	97282	6629	1054082
DF	22413	46538	131890	33974	308085	4672	33074	19593	4508	604747
WT	99	914	2927	1318	5826	36903	6941	715	1197	56840
AL	5098	63561	18846	69893	29388	11491	564844	143545	13689	920355
SGL	1366	23898	33736	127044	24097	290	110696	232104	11496	564727
BL	1786	18772	26192	51420	43187	992	15890	51789	16506	226534
Total (pixels)	264574	549481	3797642	954943	777784	63019	951046	656775	73587	8088851

Note: For an explanation of the symbols, see Table 1. The number underlined means that the vegetation transitions were not present.

Table 5 Summary of the change detection results

Change detection number	Change detection method	Classification method and data used	Overall accuracy (n = 97079)	Kappa (n = 97079)
1	Post-classification with 81 classes	ANN with 7 bands, DEM, slope for two individual images	65.06%	0.6096
2	Post-classification, 81 classes merged into 24 classes	ANN with 7 bands, DEM, slope for two individual images	72.94%	0.6921
3	ANN change detection with 82 sub-classes, merged into 24 classes	ANN with 8 PCA components, DEM, slope	78.42%	0.7552
4	ANN change detection with 82 sub-classes, merged into 24 classes	ANN with 8 PCA components	75.49%	0.7215
5	ANN change detection with 24 broad classes	ANN with 14 bands, DEM, slope	76.37%	0.7312
6	ANN change detection with 82 sub-classes, merged into 24 classes	ANN with 14 bands, DEM, slope	77.29%	0.742

Note: n is the number of pixels.

classes were merged into 22 change and no-change classes based on visual interpretation and field knowledge, the overall accuracy was improved about 7%, and the kappa value increased about 0.08.

The highest overall accuracy was found to be 78.89%, and the highest kappa 0.7602, for the ANN change de-

tection with 17 inputs (change detection number 4). Compared with the vegetation change map with 81 classes produced with post-classification, the overall accuracy increased 13.4%, and the kappa value increased 0.135. The overall accuracy is increased about 2.5% and Kappa value increased about 0.03 when comparing change detection numbers 3 and 4 (Table 5). In addition, if the number of ANN input layer is 15 without two extra channels (DEM and slope), the overall accuracy is 3.4% lower compared with the ANN change detection using DEM and slope as two extra bands (change detection number 4). The ANN change detection method with simulate training data yielded a quite low accuracy. The overall accuracy is 67.94%, and the kappa value is 0.6387. It is only about 3% higher than t post-classification change detection with 81 full sets of transition classes.

Figure 4 shows the change vegetation maps generated from three different change detection methods. Visual inspection suggests that using or not using slope and elevation has very little effect on the final change map derived with direct ANN change detection techniques. These two maps also are similar to the map produced using post-classification, where the 81 classes were reduced to 22 classes (Figure 4).

2.2 Results from change and no-change areas detection

As mentioned in section 1.6, in order to further analyze if the errors are due to the classification or the change detection techniques, the change detection error matrix can be collapsed into a no-change and change error matrix (Figure 5).

For the change and no-change detection, Figure 5 shows that ANN change detection yields the highest accuracy (overall accuracy = 93.78%, kappa = 0.8272). The poorest accuracy is obtained by the NDVI differencing change detection. The overall accuracy is 80.64%, and the kappa is 0.5661. For the post-classification change detection method, the accuracy of the map with 24 classes (overall accuracy = 89.41%, kappa = 0.6819) is higher than the map with 81 classes (overall accuracy = 82.67%, kappa = 0.6003).

3 Discussion and conclusions

The results show that the ANN one pass change detection method can produce higher accuracy change detection maps than the post-classification technique (Table 5). After the 81 possible vegetation transitions were reduced to 24 classes (with removal of transitions that were not present), the overall accuracy of the post-classification technique improved by 8%, and the kappa improved by 0.09 (Table 5). This means that some of the 81 vegetation transition classes were confused, as a result of errors in the two individual classifications. The change and no-change error matrices also show that merging the 81 classes into 24 classes the accuracy of

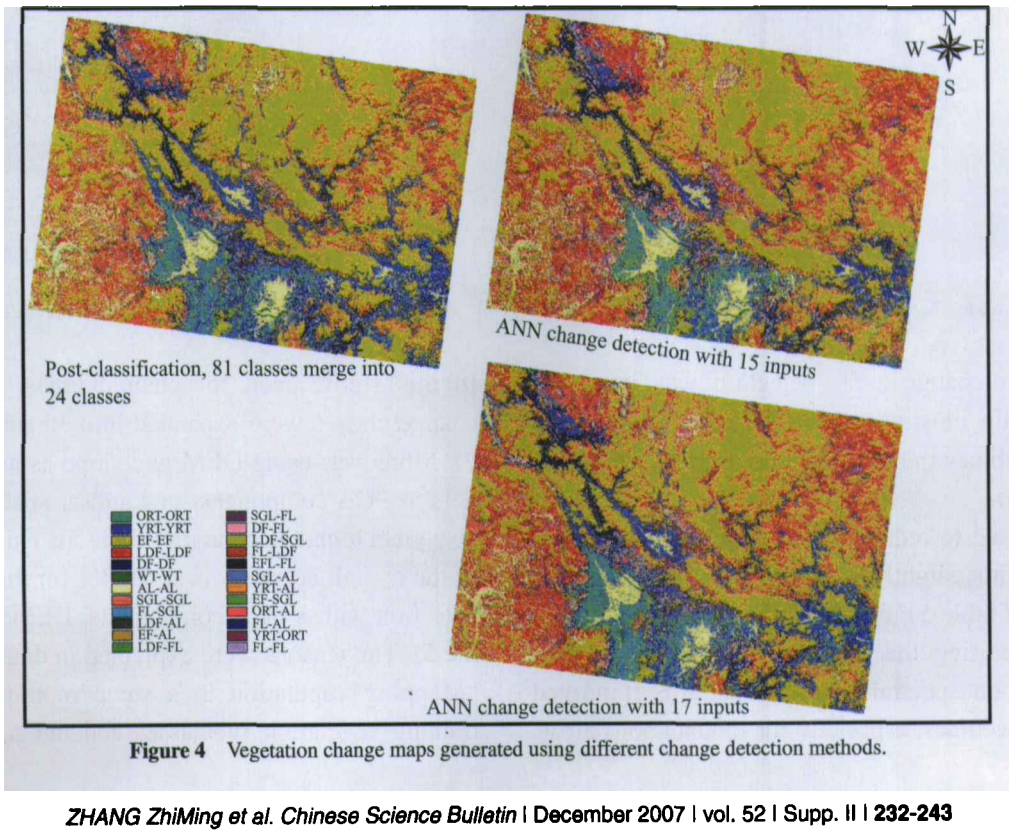

Figure 4 Vegetation change maps generated using different change detection methods.

	No-change	Change	Total
No-change	71224	3812	75036
Change	2225	19818	22043
Total	73449	23630	97079

Overall accuracy = 93.78%

Kappa = 0.8272

ANN change detection with 8 PCA components, elevation and slope

	No-change	Change	Total
No-change	56690	2036	58726
Change	16759	21594	38353
Total	73449	23630	97079

Overall accuracy = 80.64%

Kappa = 0.5661

NDVI differing change detection

	No-change	Change	Total
No-change	58873	2244	61117
Change	14576	21386	35962
Total	73449	23630	97079

Overall accuracy = 82.67%

Kappa = 0.6003

Post-classification with 81 classes

	No-change	Change	Total
No-change	71656	8489	80145
Change	1793	15141	16934
Total	73449	23630	97079

Overall accuracy = 89.41%

Kappa = 0.6819

Post-classification, 81 classes merged into 24 classes

Figure 5 Error matrices for change and no-change.

Figure 6 7-year-sold rubber trees in 2004.

Figure 7 7-year-old rubber trees in 2003.

change and no-change areas detection was improved about 7%, again illustrating that the post-classification technique combines the errors of the original classifications (Figure 5).

PCA was used to reduce the 14 TM channels into 8 PCA components, slightly improving the change detection accuracy (Table 5). For the individual image classifications, separating the vegetation classes into subclasses based on spectral response patterns improved classification accuracy, especially for mountainous areas. In this study, even for change areas, 15 vegetation change classes were expanded into 36 subclasses (Table 2). Moreover, using DEM and slope as additional channels to PCA components or Landsat spectral bands can also yield higher accuracies (Table 5). This improvement of the overall accuracy is about 3% for the ANN change detection with 8 PCA components, DEM and slope (Table 5). The reasons were explained in detail in the report "Mapping vegetation in a steep mountain terrain by training vegetation subclasses and integrating ancillary

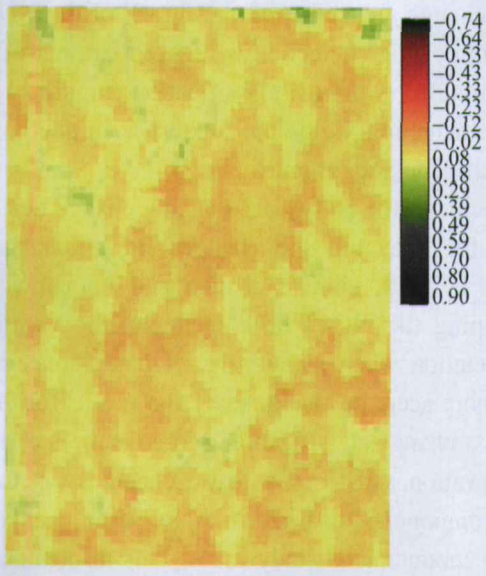

Figure 8 NDVI for 7-year-old rubber trees in 2004.

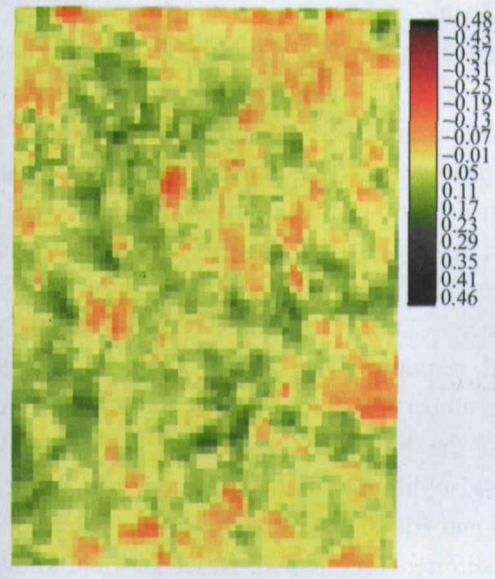

Figure 9 NDVI for 7-year-old rubber trees in 2003.

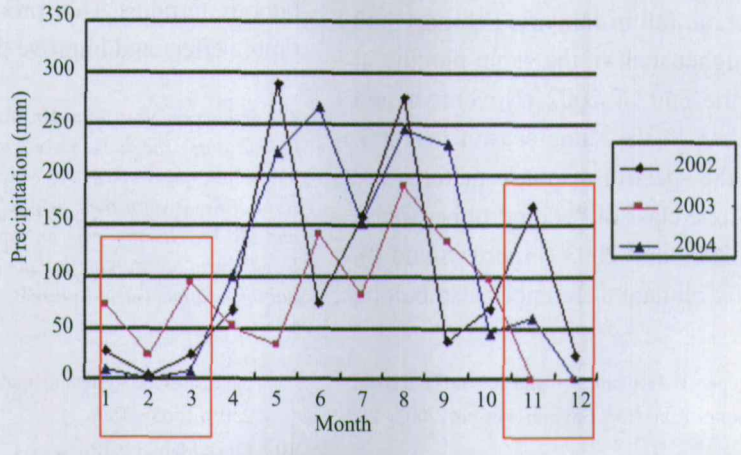

Figure 10 Precipitation for 2002, 2003 and 2004 in the study area.

	No-change	Change	Total
No-change	58487	3071	61558
Change	3927	31292	35219
Total	62414	34363	96777

Overall accuracy = 92.77%

Kappa = 0.843

ANN change detection with 8 PCA components, DEM, slope

	No-change	Change	Total
No-change	54680	3761	58441
Change	7734	30602	38336
Total	62414	34363	96777

Overall accuracy = 87.85%

Kappa = 0.7416

NDVI differencing change detection

	No-change	Change	Total
No-change	54016	6810	60826
Change	8398	27553	35951
Total	62414	34363	96777

Overall accuracy = 84.29%

Kappa = 0.6604

Post-classification with 81 classes

	No-change	Change	Total
No-change	58874	10471	69345
Change	3540	23892	27432
Total	62414	34363	96777

Overall accuracy = 85.58%

Kappa = 0.6689

Post-classification, 81 classes merge into 29 classes

Figure 11 Error matrices for change and no-change areas, including the changes caused by different climatologic conditions.

data" (Zhang 2005)[1)].

Figure 5 shows that the poorest accuracy was obtained with the NDVI differencing method. Even though the two images were acquired in the same season (March), some of changes were caused by climatologic differences. For example, the transitions "DF to DF without leaves", "YRT to YRT without leaves" and "ORT to ORT without leaves" are caused by climate differences (Table 2). Figures 6 and 7 show that the spectral response patterns are quite different for the "young rubber trees" in the 2004 and 2003 images. Because of the difference in spectral response, NDVI values are also different in the 2004 and 2003 images (Figures 8 and 9). These changes can be detected by the NDVI differencing method. Based on field knowledge, the rubber trees are about 8 years old. This means the changes are not vegetation transitions.

Figure 10 shows that rainfall in January, February and March 2003 is much higher than in the same months in 2004. The rainfall at the end of 2002 (November and December) is higher than in the same season in 2003. This can explain why the spectral response patterns are quite different for the same class of "young rubber trees" between the images in 2004 and 2003 (Figures 8 and 9). If the changes caused by climate differences also belong to the change areas, then the accuracy of the NDVI differencing change detection is higher than that of the results obtained with post-classification (Figure 11). ANN change detection yields the highest accuracy compared with other methods (Figure 11).

In general, the NDVI differencing change detection is better for detecting the change and no-change areas caused by both climate change and human activities. Combining the NDVI differencing method with visual interpretation when identifying reference areas can produce more accurate change detection results for the ANN one pass change classification. Moreover, it is effective to use elevation and slope as extra channels together with PCA components, to perform ANN-based change detection in mountainous study areas. It is also important to separate the vegetation transition classes into subclasses based on spectral response patterns, especially for mountainous terrains. This processing can reduce the topographic effect and improve the change detection accuracy.

The authors are grateful to Mr. Wang Hong and his students for their help in field work. The authors are grateful to Yang Yun, Chen Mingyong and the people who work in the Naban He Natural Reserve and Mengyang Natural Reserve for their help in field work. We thank Dr. Zhang Yiping and Mr. Xie Guoqing who provided the climate data. We thank our colleagues who are working in Laboratory of Forest Management and Spatial Information, Ghent University, Belgium.

1 Lambin E F, Geist H J, Lepers E. Dynamics of land use and land cover change in tropical regions. Ann Rev Environ Resour, 2003, 28: 205−241
2 Liu J, Zhang Z, Zhuang D, et al. A study on the spatial - temporal dynamic changes of land – use and driving forces analyses of China in the 1990s. Geogr Res, 2003, 22(1): 1−12
3 Ren Z, Zhang Y. Land Use Change and Ecological Security Assessment (in Chinese). Beijing: Science Press, 2003. 3−4
4 Shi P, Jiang Y, Wang J, et al. LUCC and the Mechanism of Ecological Security Responses to LUCC (in Chinese). Beijing: Science Press, 2003. 80−151
5 Wu J. The key research topics in landscape ecology. Acta Ecol Sin (in Chinese), 2004, 24 (9): 2074−2076
6 Singh A. Digital change detection techniques using remotely sensed data. Int J Remote Sens, 1989, 10(6): 989−1003
7 Green K, Kempka D, Lackey L. Using remote sensing to detect and monitor land-cover and land-use change. Photogr Eng Remote Sens, 1994, 60(3): 331−337
8 Pat S C Jr, MacKinnon D J. Automatic detection of vegetation changes in the southwestern United States using remotely sensed images. Photogr Eng Remote Sens, 1994, 60(5): 571−583
9 Coppin P, Jonckheere I, Nackaerts K, et al. Digital change detection methods in ecosystem monitoring: A review. Int J Remote Sens, 2004, 25(9): 1565−1596
10 Lu D, Mausel P, Brondízio E, et al. Change detection techniques. Int J Remote Sens, 2004, 25(12): 2365−2407
11 Dai X L, Khorram S. Remotely sensed change detection based on artificial neural networks. Photogr Eng Remote Sens, 1999, 65(10): 1187−1194
12 Abuelgasim A A, Ross W D, Gopal S, et al. Change detection using adaptive fuzzy neural networks: Environmental damage assessment after the Gulf War. Remote Sens Environ, 1999, 70: 208−223
13 Chan J C-W, Chan K-P, Yeh A. G-O. Detecting the nature of change in an urban environment: A comparison of machine learning algorithms. Photogr Eng Remote Sens, 2001, 67(2): 213−225
14 Xiao P, Li D. Land use/cover change detection based on artificial neural network. Geomatics Info Sci Wuhan Univ, 2003, 27(6): 586−590
15 Gopal S, Woodcock C E. Remote sensing of forest change using artificial neural networks. IEEE Trans Geosci Remote Sens, 1996, 28(4): 540−551
16 Woodcock C E, Macomber S A, Pax-Lenney M, et al. Monitoring large areas for forest change using Landsat: Generalization across space, time and Landsat sensors. Remote Sens Environ, 2001, 78: 194−203

1) Zhang Zhiming, 2005. Mapping vegetation in a steep mountain terrain by training vegetation subclasses and integrating ancillary data. PhD Thesis. Chapter 4

17 Liu X, Lathrop R G Jr. Urban change detection based on an artificial neural network. Int J Remote Sens, 2002, 23: 2513−2518
18 Bruzzone L, Conese C, Maselli F, et al. Multisource classification of complex rural areas by statistical and neural-network approaches. Photogr Eng Remote Sens, 1997, 63(5): 523−533
19 Lillesand Thomas M, Kiefer Ralph W. Remote Sensing and Image Interpretation, 4th ed. New York: John Wiley & Sons, Inc. 2000. 572−575
20 Lyon J G, Yuan D, Lunetta R S, et al. A change detection experiment using vegetation indices. Photogr Eng Remote Sens, 1998, 64(2): 143−150
21 Mertens K C, Verbeke L P C, Wulf R R D. Sub-pixel mapping with neural networks: Real-world spatial configurations learned from artificial shapes. Proceedings of 4th International Symposium on Remote Sensing of Urban Areas (Regensburg, Germany), 2003
22 Atkinson P M, Tatnall A R L. Neural networks in remote sensing. Int J Remote Sens, 1997, 18(4): 699−709
23 Benediktsson J A, Swain P H, Ersoy O K. Neural network approaches versus statistical methods in classification of mutisource remote sensing data. IEEE Trans Geosci Remote Sens, 1990, 28(4): 540−551
24 Benediktsson J A, Sveinsson J R. Feature extraction for multisource data classification with artificial neural networks. Int J Remote Sens, 1997, 8: 727−740
25 Foody G M, Arora M K. Evaluation of some factors affecting the accuracy of classification by an artificial neural network. Int J Remote Sens, 1997, 18: 799−810
26 Lowell K, Richards G, Woodgates P, et al. Fuzzy reliability assessment of multi-period land-cover change maps. Photogr Eng Remote Sens, 2005, 71(8): 939−945
27 Congalton R G, Green K. Assessing the Accuracy of Remotely Sensed Data: Principles and Practices. Boca Raton: Lewis Publisher, 1999